■ Scientific Justification

The big picture: The buildup of galaxy mass is intimately linked to the metal content of galaxies because metals are a by-product of the star formation activity. Metallicity gradients (i.e. element abundance distribution throughout a galaxy) are important diagnostics of galaxy evolution, because they record the history of events such as mergers, gas inflows, and star formation histories (e.g. Maiolino & Mannucci+19). **Hence, accurate determination of element abundances for various galaxy populations through cosmic time is a key observational goal in order to understand galaxy evolution.** One of the key manifestations of the symbiotic relationship between galaxies and their metal content is the well-known mass-metallicity relation (MZR e.g. Tremonti+04, Maiolino & Mannucci+19, Curti+20) and the more recent mass-metallicity gradient relation (e.g. Baker+23).

With $L_{IR} > 10^{12} L_{\odot}$, ultraluminous infrared galaxies (ULIRGs) are amongst the most massive star-forming galaxies, the result of merging between gas-rich progenitors. Because of their proximity they are are the perfect laboratories for studying the evolution of Starburst and AGN and for testing models of galaxy formation through merging (e.g. Hopkins+13, Hayward+14). Metallicity and metallicity gradients are an integral part of such models as they trace gas flows (e.g. Davé+12). Early studies of the ULIRG element abundances based on optical emission lines, typically subject to heavy dust extinction (Rupke+08), found that ULIRGs lie below the MZR with significant implications for their mass-assembly mechanism. That ULIRGs are lacking in heavy elements is odd because galaxy merging is often accompanied by gas compression, resulting in enhanced star formation, and subsequent formation of dust and heavy elements via type II supernovas (e.g., Kilerci Eser+14).

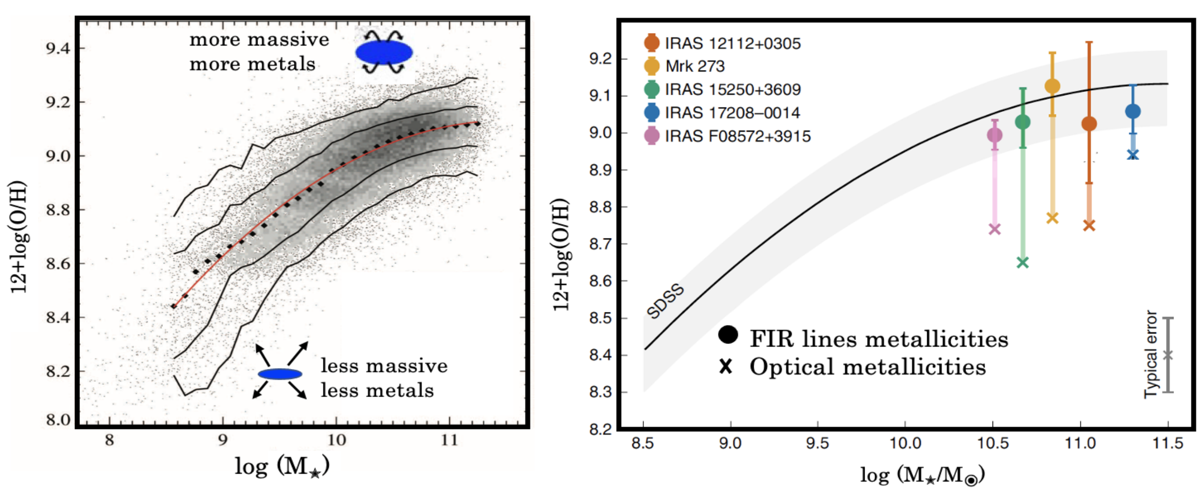

Figure 1: **Left:** The Mass-Metallicity Relation based on SDSS galaxies (Termonti+04). The solid lines are the contours enclosing 68% and 95% of the data. The red line shows a polynomial fit to the data.
Right: MZR of ULIRGs whose metallicities were measured using optical (crosses) and FIR spectral emission lines (filled circles). The black line represents the MZR for local star-forming galaxies (reproduced from Chartab+22).

More recently, Pereira-Santaella+17 and Herrera-Camus+18 found that ULIRG gas-phase metallicities determined from far-infrared (FIR) fine structure lines result in values that are much closer to those expected from the mass-metallicity relation. Indeed, Chartab+22 used SOFIA/FIFI-LS observations of FIR fine structure lines to determine gas-phase metallicities in five ULIRGs and found that ULIRGs are following the mass-metallicity relation albeit with significant uncertainties (Fig. 1, right). Their finding is certainly encouraging **but the study has two major limitations that we plan to address with the current proposal:**

• First, the determination of abundances from FIR lines is based on photoionization models from CLOUDY (e.g. Pereira-Santaella+17) or empirical correlations between U (the ionization parameter) and O/H (e.g. Fernandez-Ontiveros+22) and are thus sensitive to model assumptions and/or the samples used to derive the correlations. **With MIRI-MRS we will use the direct method to determine abundances from a combination of mid-infrared fine structure and hydrogen recombination lines.** Advantages of the direct method include the very low extinction of the MIR lines and the non-dependence on variations in electron temperature and density (e.g. Wu+08, Bernard-Salas+09). The sensitivity afforded with MIRI-MRS is crucial in detecting H recombination lines such as Pf_α 7.46 μm and Hu_α 12.4 μm (see Discussion in Technical Justification). Figure 3 shows the MIRI-MRS spectrum of VV114E (from ERS 1238) with the ionic and H recombination lines required for the study clearly marked.

• Second, to date there are no spatially resolved measurements and metallicity gradients for ULIRGs. As a result, we cannot study the mixing and re-distribution of heavy elements in ULIRGs and potentially trace gas flows as the merger progresses. **MIRI-MRS will produce spatially resolved metallicity maps that will be used to determine gradients.** Such measurements are key to test the predictions of theoretical models for merging of massive galaxies like the ULIRGs and their high-z counterparts, the submm-luminous galaxies (e.g. Naab & Ostriker+17).

Finally, by *stacking ULIRG Spitzer spectra* Veilleux+09 found that ULIRGs show an overabundance in Ne relative to the solar value, a fact that is further highlighting uncertainties and complexities in measurements of the metal content of ULIRGs.

This proposal: We propose MIRI-MRS spatially resolved spectroscopic observations of a representative sample of local ULIRGs to measure directly *neon, argon* and *sulphur element abundances and determine their spatial distribution*. Using ionic lines such as [NeII], [NeIII],[NeV],[NeVI], [ArII],[ArIII], [ArV], [SIV] and [SIII] combined with hydrogen recombination lines (Pfα, Huα) we will derive *for the first time direct* resolved element abundances and metallicities in ULIRGs.

These measurements will facilitate the study of the impact the merging of two equal mass galaxies has on the element abundances of the system. Metallicity gradients will be used to trace gas flows to/from the nuclear region of ULIRGs. We expect flatter metallicity gradients for more advanced mergers or fully coalesced systems as the result of the inflow of metal-poor gas from the outskirts of the galaxies (e.g. Sharda+21, De Lucia+20). The proposed investigation will have significant impact on our understanding of dusty interacting/merging systems at high redshifts (where similar studies are not possible) and the mixing and redistribution of heavy elements in mergers compared to predictions of merger models.

What is the real metal content of ULIRGs ? With $L_{IR} > 10^{12} L_\odot$, ULIRGs are amongst the most intensely star-forming galaxies in the Universe and because of their relative proximity they are ideal targets to study the merging process and its impact on the distribution of elements and galaxy evolution. Theoretical models and numerical simulations (e.g. Montuori+10, Rupke+10, Torrey+12, +19, Sharda+21) postulate that as a result of tidal forces acting on interacting galaxies, the nuclear metallicity can be substantially depressed by gas inflows causing the metallicity gradient to flatten. Kewley+06, +10 compared the nuclear gas-phase metallicities of nearby field galaxies with nearby galaxy pairs and found that close pairs have systematically lower metallicities than either field galaxies or more widely separated pairs at the same luminosity. Although Chartab+22 (Fig.1 right), find that ULIRGs are not 'underabundant' for their mass (i.e. lying below the MZR), their result cannot be easily compared to the predictions of theoretical models. The study finds that all ULIRGs have the same abundances irrespective of merger stage (model predictions and numerical simulations state that advanced mergers should have depressed nuclear metallicities due to metal-poor gas inflows). This may be due to the fact that the datasets used for the study comprise *unresolved* observations with SOFIA/FIFI-LS (see Fig. 4 for a comparison of the JWST data with those from SOFIA-/FIFI-LS). Therefore, it is impossible to investigate differences in the metal content for different stages of interactions and, more importantly, study galaxy metallicity gradients. In addition, the observations have targeted only a handful of ULIRGs most of them at advanced merger stages and at the high end of the luminosity distribution.

The main goals of this proposal are:

1) Determine element abundances using multiply-ionised fine structure lines:

Diagnostics: Pf_α, Hu_α, [NeII], [NeIII],[NeV],[NeVI], [ArII],[ArIII], [ArV], [SIV] and [SIII]

Using the strength of the MIR fine structure lines relative to the hydrogen recombination lines we will derive the abundances as well as gradients of the gas producing these emission features. Both Pfα 7.46 μm and Huα 12.4 μm can be used for the determination. Mid-infrared (mid-IR) lines offer many advantages over UV and optical lines for measuring abundances. First, many stages of the ionization of the Ne, Ar and S elements are in the mid-IR. The direct measure of important stages of ionization of these elements greatly reduces, or completely avoids the need to use ionisation correction factors (ICFs, e.g. Bernard-Salas+09), significantly reducing uncertainties and corrections. Second, the mid-IR lines have a minimal dependence on electron temperatures (as opposed to the optical and UV lines). In addition, mid-IR lines are much less affected by extinction.

2) Investigate resolved metallicity gradients and their link to galaxy properties:

Diagnostics: as in (1)

Our sample (see discussion below) has been carefully selected to include objects in a variety of interaction stages from well separated interacting galaxies to fully coalesced objects. We will therefore search for variations in the metallicity gradients as a function of interaction stage. We expect a flattening of the metallicities as we progress from widely separated pairs to merging and finally fully merged systems. Flat metallicity gradients in the most advanced mergers (fully coalesced systems) would be the result of depressed nuclear metallicities caused by possible inflows of metal-poor gas towards the nuclear regions and/or removal of metals due to outflows (e.g. Sharda+21).

3) Investigate the link between the multiphase ISM and metallicity gradients

Diagnostics: Pf_α, Hu_α, *ionic lines,* H_2 *rotational lines, PAH bands, HCN,* C_2H_2.

Using H recombination lines, ionic fine structure lines, H_2 molecular lines and PAHs we will determine the physical condition and spatial extent of the ionized, molecular and neutral ISM and investigate the link with the chemical conditions in ULIRGs. In particular, we will link the kinematics, as derived from H_2 rotational and H recomb. lines betraying inflows/outflows with the derived metallicity gradients. With these resolved abundance studies we will search for differences in the gas-phase metallicity gradients amongst ULIRGs at various stages of interaction, unveiling the physical processes that shape them (e.g. Sanchez+14). This would be the first study linking the ISM, SFR, to metallicity gradients in ULIRGs.

4) Measure obscuration:

Diagnostics: Sil. absorption (9.7 & 18 μm), Hu_α, Pf_α

With dust obscuration reaching $A_V \sim 35$ mag or $A_{MIR} \sim 1.5$ mag (Chiar+06) careful determination of the extinction towards the nuclear regions of ULIRGs is necessary. For this purpose, we will measure the extinction, as a function of distance from the centre, based on the depth of the silicate absorption band (e.g. Donnan+23a). In addition, the ratio of two H recombination lines in the MIRI-MRS range will also give a reliable measure of the extinction. Appropriate corrections will be applied where necessary.

To achieve these observational goals, we request high-spatial resolution mid-infrared MIRI/MRS integral field spectroscopy for a representative sample of ULIRGs with a wealth of ancillary data (including ALMA CO (2-1) and continuum and VLT/MUSE archival data). The proposed observations will spatially and spectrally resolve the integrated Spitzer spectra by a factor of $\sim 10\times$ in spatial and a factor of $\sim 30\times$ spectral resolution which is an imperative in order to achieve our goals. The proposed MIRI/MRS observations of a representative sample of ULIRGs in terms of interaction stage, nuclear activity, and luminosity will provide solid observational constrains on the effects of mergers in the evolution of galaxies.

The ULIRG sample: We selected a representative sample of nearby ($z < 0.1$; <460 Mpc) ULIRGs to cover the most relevant parameters needed to characterize the metal content of ULIRGs during the merger process: (1) the interaction stage (from interacting pairs to advanced/fully-coalesced mergers); (2) dominant activity classification (AGN vs. SF); and (3) the IR luminosity (from $12.0 < \log L_{\mathrm{IR}} < 12.8$).

The proposed sample is drawn from the 1 Jy ULIRG sample (Kim & Sanders+98) consisting of ULIRGs selected at 60 μm with $z<0.3$. For the present study we limit the redshift to $z<0.1$ as we are interested in spatially resolving the fine structure line emission for all the sources in order to determine metallicity gradients. Fig. 2 shows the targets culled from the parent sample. The proposed targets were selected to: (i) include systems in a wide range of interaction stages and (ii) showing evidence of extended emission as we are keen to measure gradients. The proposed targets are shown in red. The four pre-merger

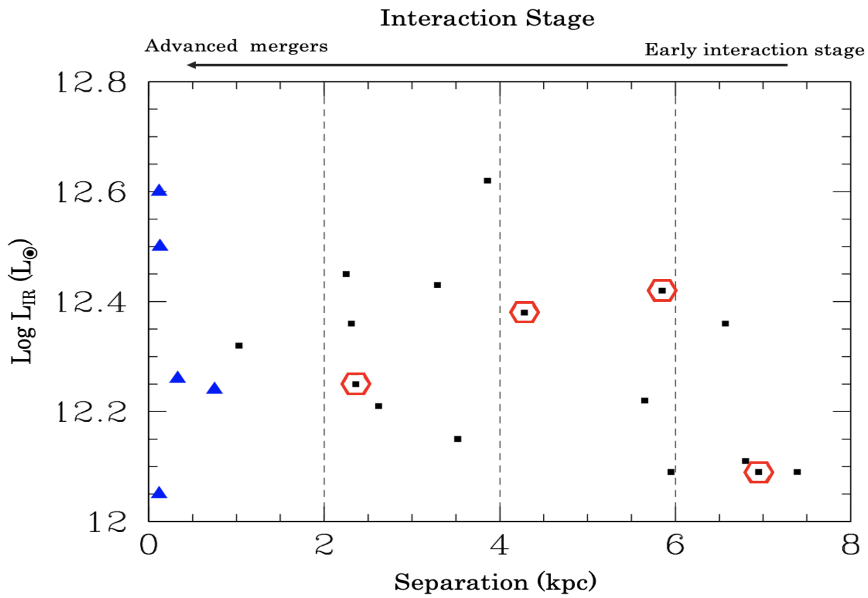

Figure 2: The sample selection. Targets with large red hexagons are the ones that will are proposed here. Targets in blue are/will be observed as part of GTO/Cycle 1.

systems (8 nuclei in total) were selected for the availability of high resolution ALMA and VLT/MUSE archival data. For the analysis we will include objects from GTO1 programs (IDs 1267 and 1268) and GO1 program (ID 1717 which has no proprietary time) which are shown in blue, no observations are available so far. With this proposal, we will complete the JWST archival observations, which only include advanced mergers, with interacting systems. This is essential for tracing the evolution of metals during the merger process. Hence, the final sample consists of 9 systems, 4 of which are proposed here. We note that the analysis will consist of 13 nuclei as the proposed targets are all interacting. We note that no MRS spectra of ULIRGs are currently available in the JWST archive, however, in Figure 3 we show MRS spectra from a LIRG (VV114E) from ERS ID 1328 (see Tech. Justification). **From the local to the distant Universe:** Although local ULIRGs are rare, their number density rises rapidly, reaching a density of several hundreds per sq. deg. at z∼1. The proposed study in local ULIRGs is important as they are considered local analogous of the high-redshift (z>2) merger submillimetre galaxies showing elevated SFRs and star-formation efficiencies (SFE=SFR/M(H2)) (e.g., Tacconi+20). Consequently, understanding the baryon cycle in low-redshift ULIRGs becomes crucial since they connect to the stellar history and super-massive black hole mass of galaxies that dominate the peak of the SFRD.

Technical Justification

Instrument selection: We request MIRI/MRS observations of a representative sample of 9 (4 new plus 5 archival) local ULIRGs (Table 1) over the full spectral range from 4.9 to 28.3 μm. We choose the Medium Resolution Spectroscopy (MRS) mode that provides a spectral resolution of 80 – 220 km s^{-1} and a spatial resolution of 0.27 – 0.7 arcsec (corresponding

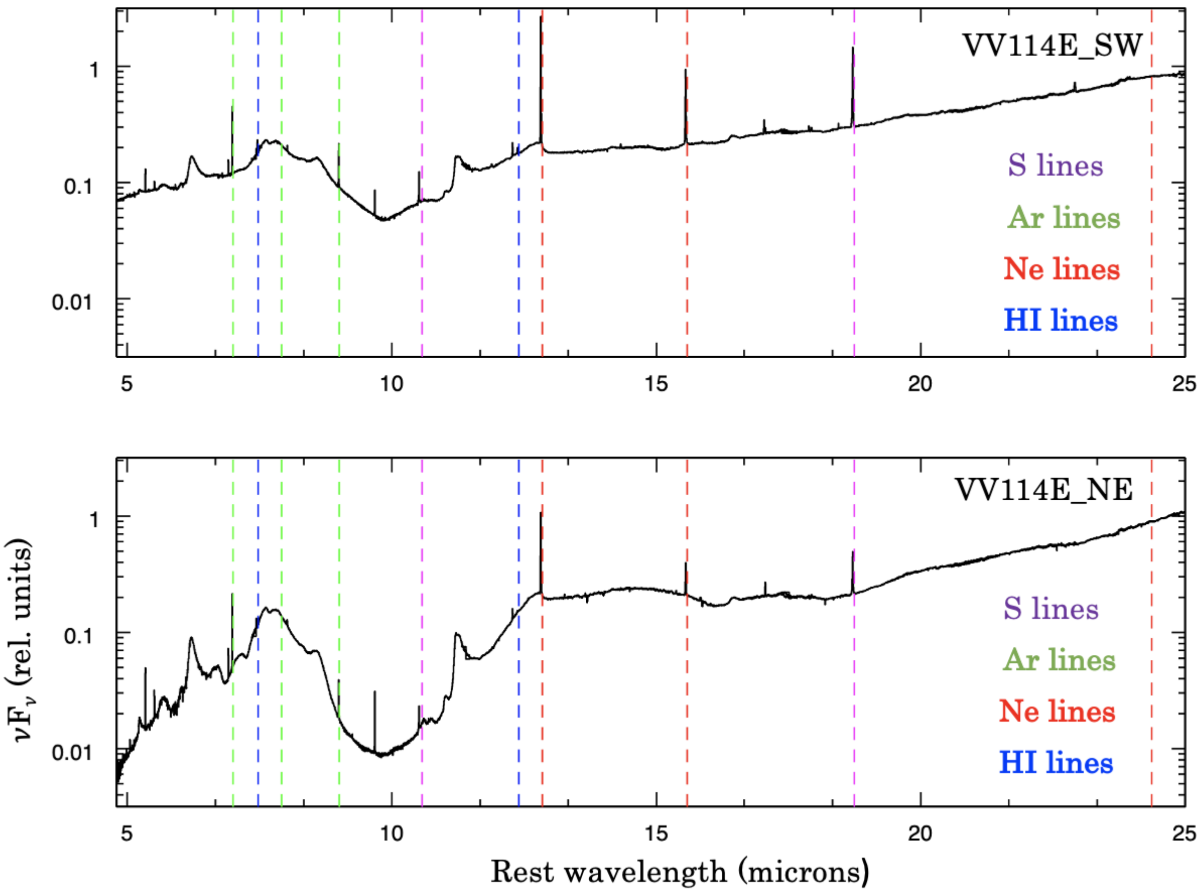

Figure 3: MIRI-MRS spectra of VV114ESW (top) and VV114ENE (bottom) nuclei extracted with a 1" circular aperture showing the HI, S, Ne and Ar lines that are essential for the proposed study. The data shown are archival data from ERS ID 1328.

to 250 – 680 pc at the distance of our targets) absolutely essential to achieve our goals. Since local ULIRGs experience significant dust-obscuration (often reaching $A_V \sim 35$ mag or $A_{MIR} \sim 1.5$ mag, Chiar+06), observing in the MIR is crucial.

Spectral & Spatial Setup:

The emission lines needed to determine element abundances are distributed across the entire MIRI-MRS spectral range, therefore, we request observations utilising the three MRS sub-bands. In addition, we will use H_2 rotational lines (S(1) to S(9)) to measure the spatial extent of the warm gas and the PAH bands (at 6.2, 7.7, 8.6, 11.3 and 17 μm) to trace SF regions. Figure 3 shows the spectra of the IR luminous galaxy VV114E taken from the JWST archive (part of ERS ID 1328). VV114E is a z=0.0207, D=84 Mpc $L_{IR} = 10^{11.71}$ $L_\odot$ galaxy, in the mid-stage of a major merger (e.g. Rich+23, Donnan+23b). It is therefore, not too dissimilar from the ULIRGs that we propose to observe here.

Most of the activity in local ULIRGs takes place within a few kpc. The spatial resolution afforded by MIRI-MRS is essential to resolve the emission in the nuclear and inner disk

Table 1: The sample targets

NAME	z	log L_{IR} $L_\odot$	Separation[a] kpc	Int. Class[b]	Sp. Type	Notes
12112+0305	0.073	12.38	4.28	Pre-M	HII	2x MIRI pointings
14348-1447	0.083	12.42	5.85	Pre-M	L	2xMIRI pointings
22491-1808	0.078	12.25	2.36	Pre-M	HII	2x MIRI pointings
10190+1322	0.076	12.09	6.57	Pre-M	L	2x MIRI pointings
UGC 5101	0.039	12.05	<0.12	Ad-M	L	GO1/ID1717
17207-0014	0.043	12.50	<0.13	Ad-M	HII	GO1/ID1717
Arp 220	0.018	12.26	0.33	Ad-M	L	GTO1/ID1267
Mrk 273	0.038	12.24	<0.72	Ad-M	S2	GO1/ID1717
Mrk 231	0.042	12.60	<0.12	Ad-M	S1	GTO1/ID1268

[a]:Projected nuclear separation from Veilleux+02

[b]:Interaction class: Pre-M: two nuclei are identifiable, Ad-M: separation between the interacting nuclei is <1 kpc or have nuclei have coalesced.

regions of the ULIRGs. At the median distance of our sample ($\sim$ 360 Mpc), the field of view of the smallest MRS channel (Channel 1) covers 4-9 kpc and contains much of the region that we are interested in observing. In Figure 3 we show the MIRI channel 1 FOV superimposed on the ALMA CO(2-1) map of one of our targets 12112+0305. The spatial resolution of the ALMA map (0.4 arcsec) is well matched to MIRI-MRS spatial resolution (0.25-0.7 arcsec) at the distance of our sample. In the same Figure we show the FIFI-LS [OIII]52μm map of the same target for comparison (this is taken from Chartab+22) with a resolution of 9"/pixel.

Since we expect the emission to be spatially extended we request a 4-point dither for our sources. This will enable cosmic rays and bad pixels removal and better sampling of the PSF for our science targets. We chose a 4-point dither pattern for the target observations and a 2-point dither pattern in the dedicated background observations. This will enable cosmic rays and bad pixels removal and better sampling of the PSF in the case of the science targets.

We also request dedicated background observations with the same exposure times at 2 dither positions to enable background subtraction for the extended emission of our targets (following JWST helpdesk recommendations). All of the four targets we propose here are interacting pairs with large nuclear separations and require two pointings, one for each nucleus.

Observing Strategy & Exposure Time Calculations:

Figure 4 shows the FOV of MIRI/MRS channel 1 overlaid on the CO(2-1) ALMA map of one of the proposed targets, IRAS12112+0305. We base our exposure time estimates on existing Spitzer/IRS and IRAC 8μm observations of our sample galaxies. Our overall integration times are driven by the need to obtain sensitive measurements of the MIR fine structure lines as well as the hydrogen recombination lines Pf_α and Hu_α in both nuclei of

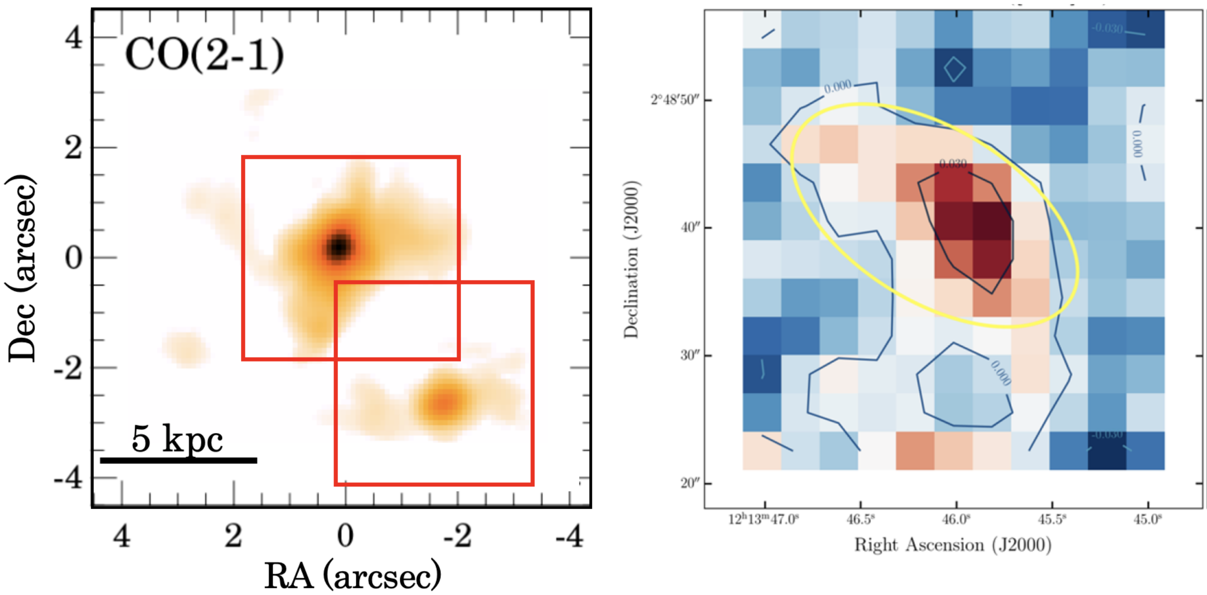

Figure 4: ALMA CO(2-1) map of 12112+0305 with the MIRI-MRS Channel 1 FOV in red (left panel). The CO(2-1) map is from the ALMA archive (but also published in Pereira-Santaella+18), the scale of the ALMA map is shown at the bottom left of the Figure. On the right panel we show the [OIII]52μm map of the same source (12112+0305) observed with SOFIA/FIFI-LS with a spaxel size of 6 arcsec.

our systems. The ratios of $Pf_\alpha/H_\alpha \sim 9.0\times10^{-3}$ and $Hu_\alpha/H_\alpha \sim 3.5 \times10^{-3}$ (from Hummer & Storey+87) have been used to ensure that the lines will be detected with enough sensitivity ($>$10 σ) throughout each of the nuclei. The integration times are determined by assuming that our sources comprise a central nucleus (point-source like) and an extended component (SF disk) with a flat distributed extended emission. We have assigned 30% flux to the disk based on decomposition of the MIR spectra of our targets (Hernan-Caballero+15). It is worth stressing that since we are interested in detecting *extended emission* we have set up the scenes in the ETC to ensure a S/N of at least $\sim 5\sigma$ for the continuum and $>10\sigma$ for lines in the extended regions. According to the ETC, on-source integration times of 1054 sec for each MRS sub-band are required to achieve our goals. The total requested science time is 8.8 h.

References:

- Baker, W.M., et al., 2023, MNRAS, 519, 1149
- Bernard-Salas, J., et al, 2009, ApJS, 184, 230
- Chartab, N., et al., 2022, Nat. As. 6, 844
- Chiar, J.E., et al., 206, ApJ 637, 774
- Curti, M., et al., 2017, MNRAS, 465, 1384
- Davé, R., et al., 2012, MNRAS, 421, 98
- De Lucia, G., et al., 2020, MNRAS, 498, 3215
- Donnan, F. et al., 2023b, MNRAS, 519, 3691

- Donnan et al., 2023a, A&A in press
- Fernandez-Ontiveros, J., et al., 2021, A&A, 652, 23
- Hayward, C., et al., 2014, MNRAS, 442, 1982
- Hernan-Caballero, A., et al., 2015, ApJ, 803, 109
- Herrera-Camus, R., et al., 2018, ApJ 861, 95
- Hopkins, P. F., et al., 2013, MRAS, 430, 1901
- Hummer, D.& Storey, G. 1987, MNRAS, 224, 801
- Kewley, L., et al., 2010, ApJ, 721, 48
- Kewley, L., et al., 2006, AJ, 131, 2004
- Kilerci Eser, E., et al., 2014, ApJ, 797, 54
- Kim and Sanders 1998, ApJS, 119, 41
- Maiolino, R. & Mannucci 2019, AARA, 27, 3
- Montuori, M., et al., 2010, A&A, 518, 56
- Naab, T., & Ostriker, J., 2017, ARA&A, 55, 59
- Nardini, M., et al., 2008, MNRAS, 385, 130
- Pereira-Santaella, M. et al., 2021, A&A, 651, 42
- Pereira-Santaella, M., et al., 2017, MNRAS, 470, 1218
- Perna, M., et al., 2021, A&A, 646, 101
- Rich, J., et al., 2023, arXiv:2301.02338
- Rigopoulou, D., et al., 1999, AJ, 118, 2625
- Rupke et al., 2010, ApJ, 710, 156
- Rupke et al, 2008, ApJ, 674, 182
- Sharda, P., et al., 2021,MNRAS, 506, 1295
- Tacconi, L., et al., 2020, ARAA, 58, 157
- Torrey, et al., 2019, MNRAS, 484, 5587
- Torrey, et al., 2012, ApJ, 746, 108
- Tremonti, C., et al., 2004, ApJ 613, 898
- Wu, Y., et al., 2008, ApJ, 673, 193

Special Requirements (if any)

Justify Coordinated Parallel Observations (if any)

Justify Duplications (if any)

Analysis Plan (AR only)